Available online at www.sciencedirect.com
SCIENCE DIRECT
Journal of Sound and Vibration 297 (2006) 227–242
JOURNAL OF SOUND AND VIBRATION
www.elsevier.com/locate/jsvi

Experimental studies of quasi-longitudinal waves power flow in corrugated plates

Nirmal Kumar Mandal*

Centre for Railway Engineering, Central Queensland University, Bruce Highway, Rockhampton, Queensland 4702, Australia

Received 20 September 2004; received in revised form 20 February 2006; accepted 27 March 2006
Available online 27 June 2006

Abstract

The structural intensity technique using cross-spectral densities is used to estimate the quasi-longitudinal wave power in rectangular and trapezoidal corrugated plates in the frequency domain. The two-point transducer method for in-plane power in naturally orthotropic plate, whose thickness is uniform, is used for measuring in-plane vibration power transmission of these plates. The method of elastic equivalence is used to facilitate power flow estimation. It is also necessary to re-model the trapezoidal corrugated plate to rectangular corrugated plate so as to apply the method of elastic equivalence. An isotropic plate is also used for this measurement. Measured in-plane power flow from corrugated plates is compared to that from isotropic plate. The effects of in-plane stiffness on vibration power flow are also investigated.

In-plane power flow is observed to reduce gradually as the frequency increases. The effects of in-plane stiffness of the plates on quasi-longitudinal wave power are insignificant in the frequency range of interest. Some negative values of power are also observed at some frequencies at lower range.

1. Introduction

Measurements of bending wave power in beams and plates have a great significance. This type of wave contains most of the vibration energy. It is due to the fact that the excitation causing flexural waves gives transverse displacement (out-of-plane) of points on the structures which in turn greatly disturb the surrounding medium, leading to increased structure-borne noise. It is therefore necessary to address the out-of-plane excitation for flexural waves. As in the case of longitudinal waves, displacement of a point however takes place in the plane of the structures. Poisson's contraction plays a minor role to produce out of plane disturbances, causing small disturbances to the surroundings. Given this, different analysis, experiments, instrumentation, etc. were undertaken concerning bending waves, with less effort being given to the longitudinal waves. Nilsson [1] carried out a typical example of an analysis including out-of-plane motion only. That author studied a scale model of a ship structure. The calculations agreed well with experiments suggesting that the inclusion of in-plane waves did not seem to be necessary. A similar conclusion was also reached by Gibbs and Gilford [2] and Landmann et al. [3]. Gibbs and Gilford [2] showed that neglecting the

*Tel.: +617 4930 9287; fax: +610 4930 6984.
E-mail address: n.mandal@cqu.edu.au.

0022-460X/$ - see front matter © 2006 Elsevier Ltd. All rights reserved.
doi:10.1016/j.jsv.2006.03.051

in-plane waves makes little difference between statistical energy analysis (SEA) predictions and experimental results within the frequency range 400 Hz–12.5 kHz to the building structures. In the case of coupled plate structures which are joined at an angle and on which transverse exciting forces are applied, in-plane waves come out with the flexural waves since the incident flexural waves are partially converted to in-plane waves at the joint part [4]. In high-frequency range, mode of power transmission through structures by longitudinal waves may however produce a significant value [5–7]. Gibbs and Craven [8] have shown by using an energy flow method that once a flexural wave impinges on a junction, some parts are converted into an in-plane wave and it can travel through several junctions before converting back to a bending wave. Thus it may not be appropriate to neglect the contributions of in-plane waves in a SEA model. Measuring bending wave power flow in a beam that has a significant level of longitudinal wave flow can provide inaccurate results particularly when techniques using measurements on only one side of the beam are used [9]. Kay and Swanson [9] presented an analysis of how much error might occur if only flexural waves were considered in the presence of in-plane waves in beams. Craik and Thancanamootoo [10] have investigated the effects including in-plane waves in an SEA model of a building, and shown that the omission of in-plane waves will result in a large discrepancy in the prediction at remote parts of the structure, but close to the source the differences are small. Previous works suggested that omission of in-plane waves yields less discrepancy between theoretical estimation and experimental results in simple structures. But especially at the higher frequency range of complex structures, it is necessary to include the contributions of in-plane waves in structures [6].

Pure longitudinal waves, whose direction of particle displacement coincides with the direction of wave propagation, can occur in structures when the dimensions of the structures in all directions are much greater than a wave-length. This in-plane wave is however seldom encountered in practical engineering structures in frequencies of interest. In most cases, at least one of the physical dimensions of the structures is smaller than the in-plane wave-length. This gives rise to a quasi-longitudinal wave [11].

Vibration power flow analysis in the area of technically orthotropic plates (corrugated plates) is very essential for practical reasons. Beam stiffened plates, plate grid structures, corrugated plates are usually used in automotive, ship, aircraft structures. This method gives a clear picture of locations of energy sources and sinks and quantifies energy transmission paths by employing vector maps. Hence, it is essential for controlling noise and vibration in industry by incorporating proper damping treatments.

Through the literature search it is identified that most of the previous works regarding in-plane vibration were confined to simple thin structures and coupled plates using different technique such as SEA, dynamic stiffness method and similar others. Little has been published on in-plane vibration power transmission using vibration intensity technique in the area of orthotropic plates especially corrugated plates. As these types of structures are very useful for industrial applications, it is most important to address the effects of in-plane vibration propagation phenomena in relation to high frequency, and the effects of in-plane stiffness on power flow for practical reasons of noise and vibration control. That is why, in this paper, vibration intensity technique is used to predict in-plane wave power flow in technically orthotropic plates to investigate flow patterns, and influences of in-plane rigidity and frequency over vibration energy transmission.

2. Theory

In this paper, power flow by quasi-longitudinal waves is estimated by the following equation. The equation is complex and was developed using cross-spectral density functions of field signals of the plate [12]:

$$P_x(f) = \frac{D_x t}{\mathrm{d}\omega^3}\ \mathrm{Im}\ \{G_{12}\}, \tag{1}$$

where $P_x(f)$ is the in-plane vibration power flow in x-direction of the plate, D_x is the longitudinal stiffness of the plate in x-direction, d is the spacing of the transducers (Fig. 1), t is the uniform thickness of the plate, ω is the angular frequency ($2\pi f$), and G_{12} is the cross-spectrum of two acceleration signals from the measurement points (Fig. 1).

The assumptions of quasi-longitudinal wave propagation for developing Eq. (1) are to be such that one strain component in the plane of plate is zero ($\varepsilon_y = 0$) and stress perpendicular to the plane of plate is also zero ($\sigma_z = 0$) [11]. Power flow in the y-direction would be zero because of zero strain in that direction. Input power

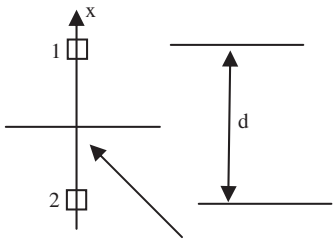

Fig. 1. Measurement point array on the plate (plate not shown).

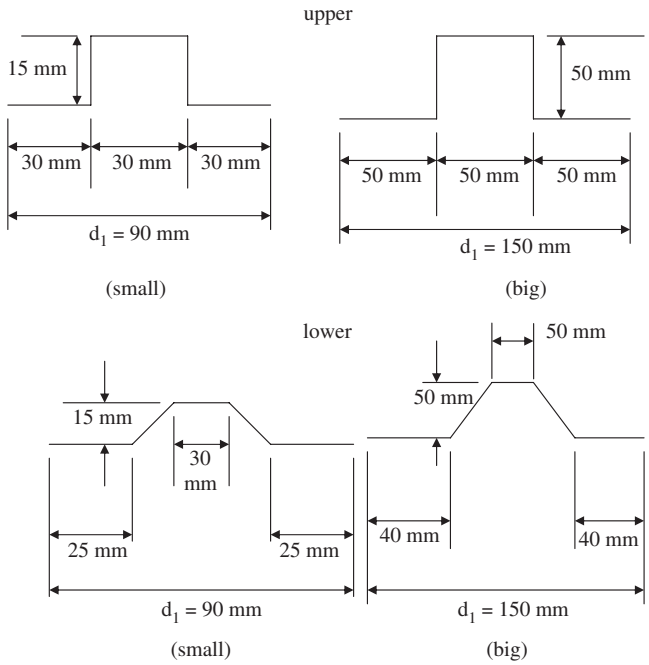

Fig. 2. Physical dimensions of cross sections of one repeating section of rectangular corrugated (upper) and trapezoidal corrugated (lower) plates for both small and big corrugation.

(P_i), on the other hand, can be obtained using Eq. (2) [13] where G_{Fa} is the cross-spectrum of force and acceleration signals:

$$P_i = \frac{1}{\omega}\ \mathrm{Im}\ \{G_{\mathrm{Fa}}\}. \tag{2}$$

3. Test rig and instrumentation

An analytical method for measuring quasi-longitudinal wave power in naturally orthotropic plates has been developed [12]. The experimental test plate models selected for the measurement of quasi-longitudinal wave power were rectangular and trapezoidal corrugated plates (Fig. 2) due to the fact that they are widely used in industries. The corrugated plates were formed from isotropic plate. Due to its geometric form of corrugation, the plate would be considered technically orthotropic. The method applicable for naturally orthotropic plates [12] could not be applicable directly to corrugated plates as their geometry is completely different (thickness is

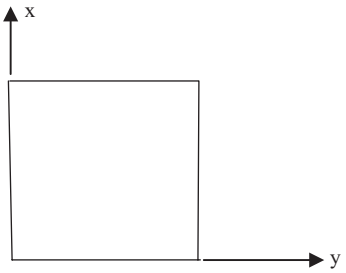

Fig. 3. Equivalent plate of uniform thickness as modeled by the elastic equivalence.

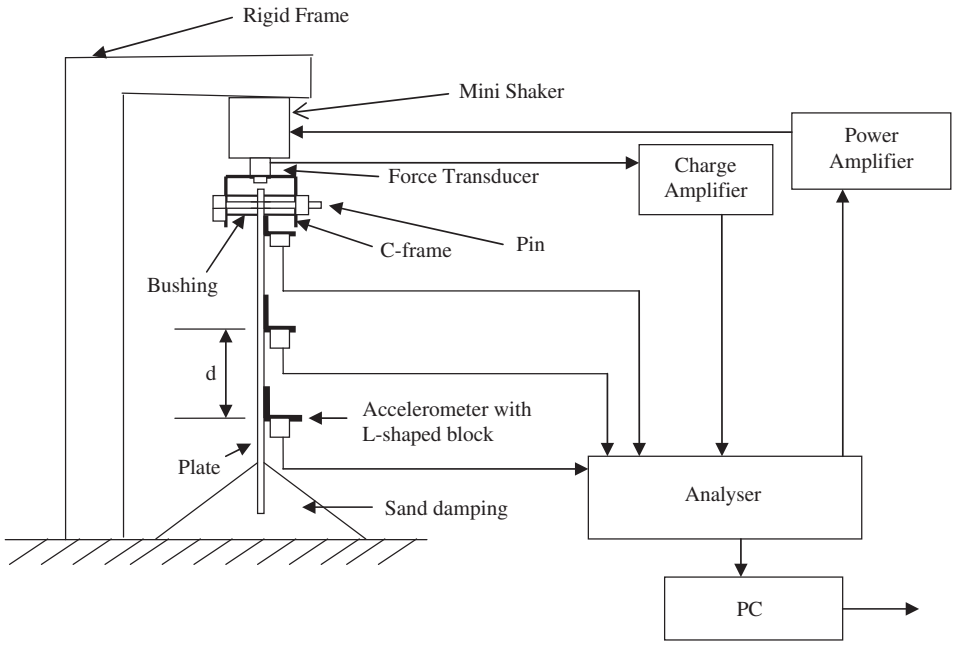

Fig. 4. Test arrangement and instrumentation for measuring quasi-longitudinal wave power in corrugated plates.

not uniform). With the help of the method of elastic equivalence [14], technically orthotropic plates (corrugated plates, Fig. 2) could be modeled to naturally orthotropic plates of uniform thickness (Fig. 3) and only then the method [12] can be applied.

A test rig (Fig. 4) for the measurement of in-plane power for plates was fabricated. Technical orthotropy was resulted due to form shape of the plate. Size of all plates is square (0.9 m × 0.9 m) with 0.8 mm thickness. One repeating section of corrugated plates is shown in Fig. 2. There are 10 such sections in small corrugated plates and six in big corrugated plates. The Young's modulus and Poisson's ratio of the plate material are 162.8 GPa and 0.31, respectively. The density ρ of the plate material is 6944.4 kg/m^3.

The excitation process for longitudinal wave in plates is rather complicated in comparison to that of bending wave. To apply excitation at the excitation point, an additional C-frame with a pin was used as in Fig. 4. The C-frame was connected to the force transducer with a threaded bolt. It was also connected to the test plate using the pin. Two bushings were used around the pin beside the sides of the plate to ensure no lateral motion of the plate. The pin was acting as an exciting element at the excitation point at the upper central part of the plate (Fig. 4). A mini-shaker (B&K type 4810), mounted vertically down to the rigid frame over the plate, provided random white noise given by FFT analyzer (HP 35670A) to the plate through force transducer (B&K type 8200) and C-frame. At the lower side of the plate, fine sand was used to ensure strong

end damping for suppression of wave reflections. Two sides of the test plate, parallel to x-axis and also parallel to the direction of corrugation, were fixed by as many as 12 big C-clamps on each side to ensure zero strain in y-direction as required for the boundary conditions for the in-plane wave power [11]. In addition, a few small C-clamps were also used for this purpose in between the big clamps.

One transducer, adjacent to the excitation point, was used for measuring data for input power, and another two mounted away from source and boundary were used for measuring transmitted power. L-shaped light weight aluminum blocks were used to detect acceleration signals from the surface of the plates. It is reasonably assumed that the light weight L-shape blocks do not disturb local responses of the plates. A light weight cubic block is generally used for detection of in-line responses of the structures. The loading effects of small L-shaped plate used in this measurement are less than that of cubic block and thereby its effects may be neglected. Piezoelectric miniature accelerometer (ICP, 1.7 g) and FFT multi-channel analyzer were used to detect necessary power spectrum and cross-spectral signals. The accelerometers were mounted on the L-shaped blocks and the L-shaped blocks were mounted on the plates using bee-wax. The influences of bee-wax are discussed later in discussion section. The standard data files, using ASCII code, of the measurements were transferred from analyzer to PC for post processing and the results were plotted.

4. Measurement of longitudinal wave power

The measurement method [12] is applicable to the orthotropic plate of uniform thickness (Fig. 3). This method could be applied directly to rectangular and trapezoidal corrugated plates using the method of elastic equivalence [14]. But for trapezoidal corrugated plates, first a repeating section of trapezoidal corrugated plate was modeled to rectangular corrugated plate. With the help of method of elastic equivalence, the rectangular corrugated plate section was then remodeled to equivalent plate of uniform thickness (Fig. 3) and thereby different elastic constants could be achieved [14].

The longitudinal wave velocity and wave-length of the isotropic plate, disregarding Poisson's effect, respectively, would be

$$C_L = \sqrt{\frac{E}{\rho}} \text{ and } \lambda_L = \frac{C_L}{f}, \tag{3}$$

where E is the Young's modulus of isotropic plate, f is the frequency, and suffix L stands for longitudinal. For orthotropic plate (corrugated plate), the wave velocity and wave-length could be obtained by using appropriate elastic property such as E by E_x. The value of E_x for corrugated plate in x-direction can be obtained using the method of elastic equivalence [14] such that $E_x = E_s/d_1$. The characteristic dimension d_1 of one repeating section of corrugation could be shown in Table 1 and Fig. 2 and s is the flat length of this section.

As the density ρ and Young modulus of the plate material are 6944.4 kg/m^3 and 162.8 Gpa, respectively, the wave velocity C_L for isotropic plate is 4841.83 m/s. Lower limit of the frequency range could be obtained by making wave-length λ_L equal to the side (0.9 m) of the plate. Therefore, the lower limit of frequency range using Eq. (3) is 5.379 kHz. In any frequency higher than this limit, the side of the plates is greater than a wave-length. The higher limit of measured frequency range, considering wave-length equal to the thickness of the

Table 1
Physical dimensions of one repeating section of rectangular and trapezoidal corrugated plate (big and small)

Types of plate/physical quantities	Rectangular corrugated plates		Trapezoidal corrugated plates	
	Small	Big	Small	Big
Length of one repeating section, d_1 in mm	90	150	90	150
Actual flat length of one repeating section, s in mm	120	250	111.6	232
Number of repeating sections	10	06	10	06

Table 2
Selected frequency range and distance for different plates

Types of plate	Wave velocity (m/s)	Lower limit (kHz)	Higher limit (kHz)	Selected frequency range (kHz–kHz)
Isotropic plate (IP)	4841.83	5.379	6052.29	6.4–12.8
Small rectangular corrugated plate (SRCP)	5590.86	6.21	6052.29	6.4–12.8
Small trapezoidal corrugated plate (STCP)	5590.86	6.21	6052.29	6.4–12.8
Big rectangular corrugated plate (BRCP)	6250.78	6.945	6052.29	8–14.4
Big trapezoidal corrugated plate (BTCP)	6250.78	6.945	6052.29	8–14.4

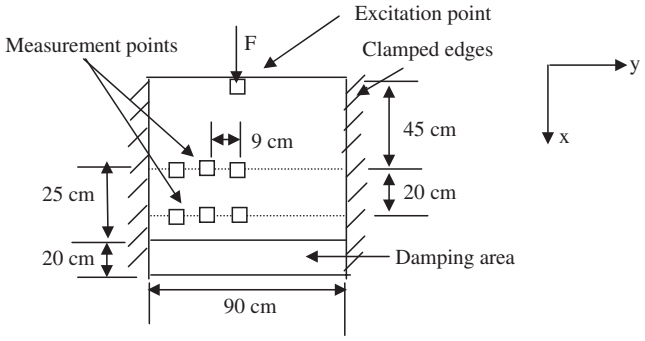

Fig. 5. Measurement line grid.

plate (0.8 mm), is 6052 kHz. From these limiting conditions, a reasonable range (6.4–12.8 kHz) is selected for isotropic plate. This range fully satisfies the conditions of quasi-longitudinal waves. Similarly, wave velocity, lower and higher limits of frequency range of each corrugated plate are computed and tabulated in Table 2. These sets of frequency ranges also satisfy the condition of quasi-longitudinal wave.

Selecting a frequency range for measurement in bending waves is different. A bending wave-length would be at least six times greater than thickness of the plates to satisfy bending waves criteria [11]. For rib or corrugated plates, the wave-length of bending wave should be significantly greater than the repeating section of the plates (Fig. 2) [11]. Satisfying all these criteria, an analysis of bending wave power measurement on rectangular corrugated plates has been carried out recently [15]. In this study, as all corrugated plates are modeled to equivalent plates (Fig. 3) of uniform cross-section, it is not at all necessary for satisfying the condition of corrugation ($\lambda \gg d_1$, length of repeated section of the plate Fig. 2). At the same time, coupling problem of waves is thereby removed.

Two sides of the plates were fixed in a manner to ensure zero strain in the y-direction. In-plane excitation was controlled such that lateral motion (perpendicular to the plate) which could disturb the detection of in-plane motion of the plates was minimized. In the measurement process, auto-spectrum and cross-spectrum between two signals were measured. The imaginary part of the cross-spectrum between force and acceleration at input point was measured as required by Eq. (2) and the cross-spectrum between two acceleration signals at different measurement points (Fig. 5) were also measured as required by Eq. (1). A mini-shaker (B&K type 4810) was used to provide input excitation, taking signals from internal noise source of the FFT analyzer (HP 35760A). A random white noise was provided to the plates. Same testing conditions relating to input force signal to all longitudinal power measurements were ensured with constant monitoring. A fixed array of transducers was considered rather than moving one transducer sequentially between the array locations. The FFT analyzer was used to collect typically 200 ensemble averages of all cross-spectra and coherence functions needed for subsequent post processing. The spectral bandwidth was set approximately to 8 Hz. The spacing (d) was selected to 20 mm. There were two measurement line grids and nine measurement points in each line (Fig. 5) for the isotropic plate and small corrugated (rectangular and trapezoidal) plates. The details of

Table 3
Measurement distances between points

Types of plate	Distances between measurement points in mm	Distances of extreme points to the edge of the plates in mm
Isotropic plate (IP)	90	90
SRCP	90	90
STCP	90	90
BRCP	75	75
BTCP	75	75

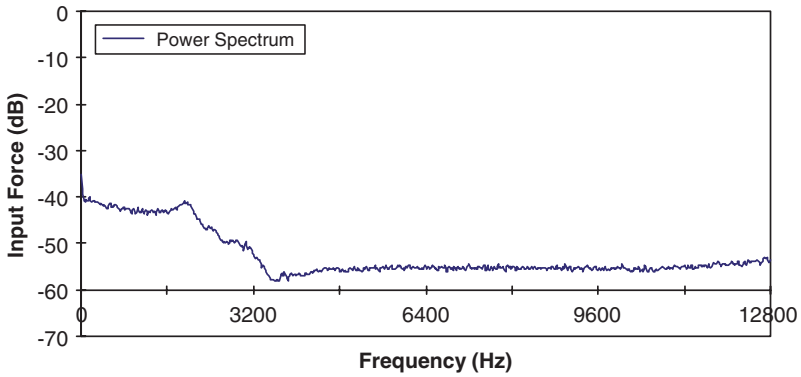

Fig. 6. Measured power spectrum of in-plane injected force (in dB) for simple isotropic plate.

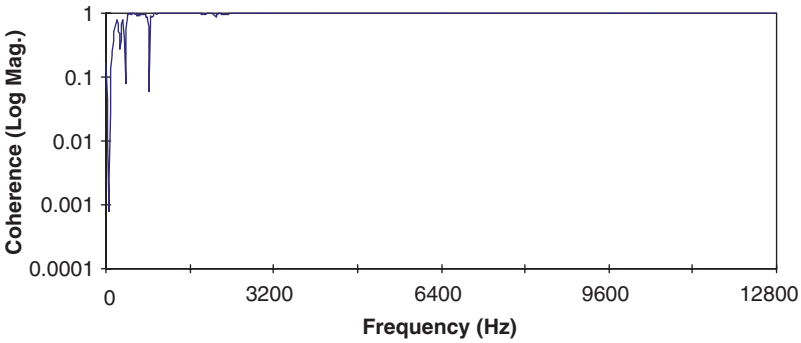

Fig. 7. Coherence function of force and acceleration at input point for isotropic plate.

distances between measurement points in each line grid, and the distances between the edges of the plates to the extreme measurement points in a line grid for all plate models are illustrated in Table 3.

Examples of input force at injected point to the isotropic plate and the coherence function between the force and acceleration signals at input are shown respectively in Figs. 6 and 7. In Figs. 8 and 9, respectively, driving point acceleration and input power injected to the plates are presented. Vibration power flow in quasi-longitudinal wave for isotropic plate from two measurement lines is also plotted in Fig. 10.

In the case of corrugated plates (rectangular and trapezoidal), data acquisitions were taken for input power, coherence function between force and acceleration at input point, driving point acceleration and power transmission. Subsequent analysis of data, as required for input power (Eq. (2)) and for power transmission (Eq. (1)), was carried out for all plates. FFT analyzer and Microsoft Excel were used to carry out the data

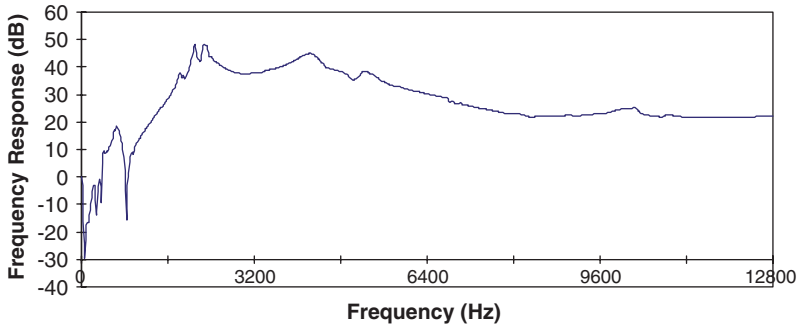

Fig. 8. Frequency response function of driving point acceleration (a/F) at input for isotropic plate.

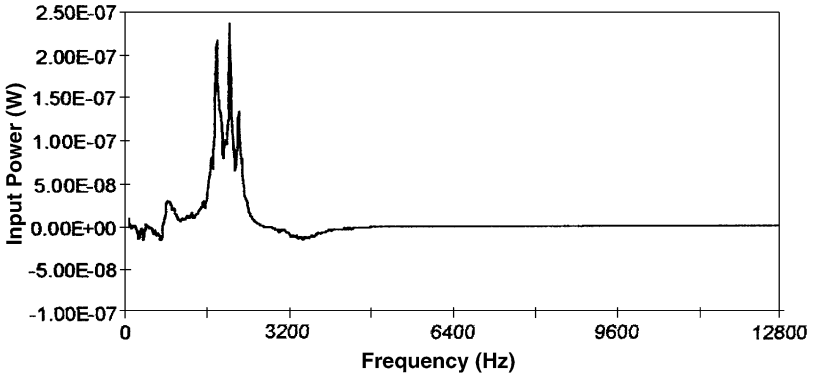

Fig. 9. Input power injected to the simple plate during data acquisition in quasi-longitudinal wave.

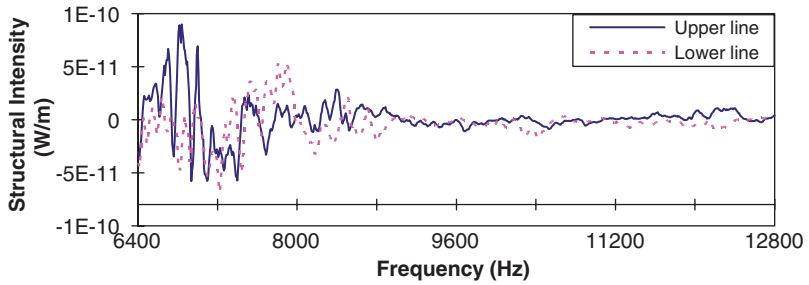

Fig. 10. Measured quasi-longitudinal wave power flow for simple isotropic plate from upper and lower measurement lines.

analysis and plotting. Interpretation of data for corrugated plates was carried out and compared with that of isotropic plate. Measurement method and test rig were also verified by comparing the trend of results of the present study with that established in literature. The following figures illustrate different aspects in this measurement: Figs. 11–14 for input power, Figs. 15 and 16 for coherence function, Figs. 17 and 18 for driving point acceleration, Figs. 19–22 for comparison of power flow from two lines, and Figs. 23 and 24 for presenting effects of in-plane rigidity on power flow.

5. Comparison and validation

When a model or a simulation is performed, it is necessary to verify it by experiments. The experimental study should be verified by other results of similar nature established in the literature. This way of verification

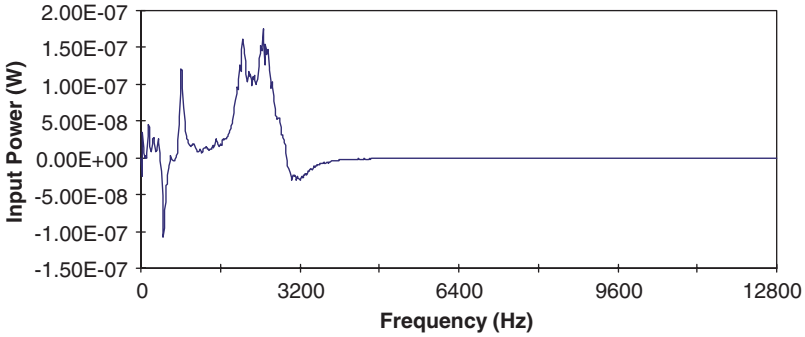

Fig. 11. Input power for small rectangular corrugated plate.

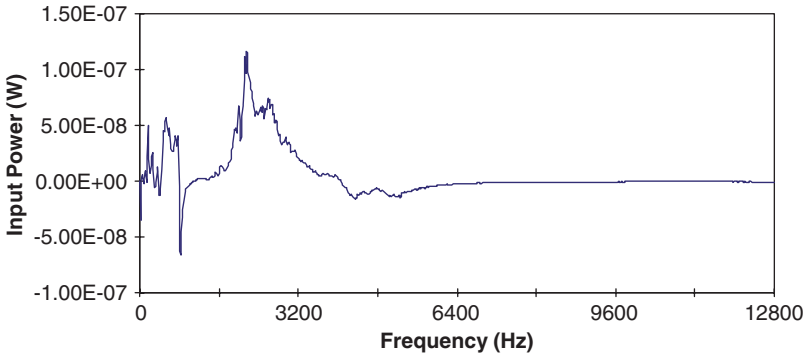

Fig. 12. Input power for small trapezoidal corrugated plate.

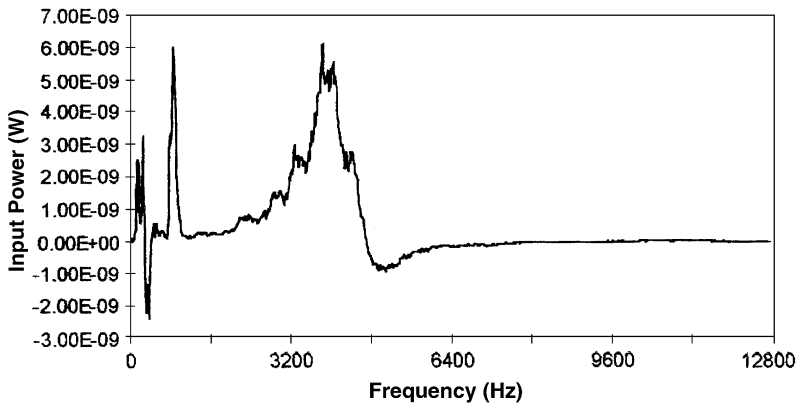

Fig. 13. Input power for big rectangular corrugated plate.

is a standard procedure [17] which is adopted here. In this paper, established measurement methods were used as tools for measuring in put power and in-plane vibration power transmission in a closed controlled condition. Through the literature search, it was identified that there are only few works of in-plane power transmission using structural intensity. In a study [5], both in-plane and out-of-plane wave power transmission were measured for L-shaped plates. Only the in-plane part of its power transmission is presented below (Fig. 25) for comparison purposes. Due to lack of precise data of that study [5], it was not possible to superimpose the graph to that of the present study. Due to unknown in-put excitation and difference in

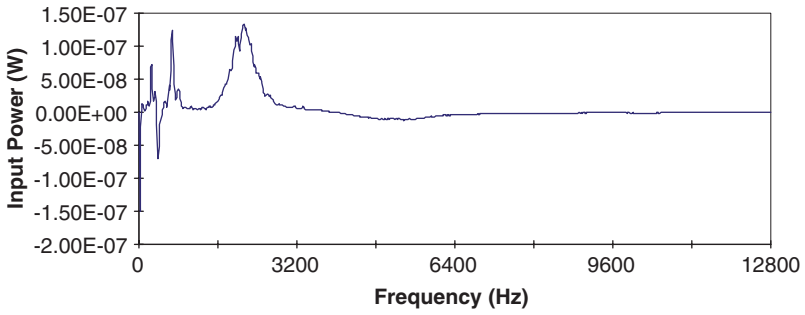

Fig. 14. Input power for big trapezoidal corrugated plate.

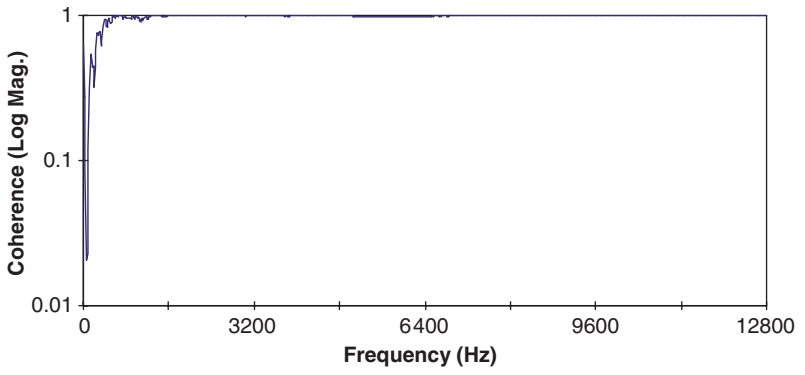

Fig. 15. Coherence between force and acceleration at input for small rectangular corrugated plate.

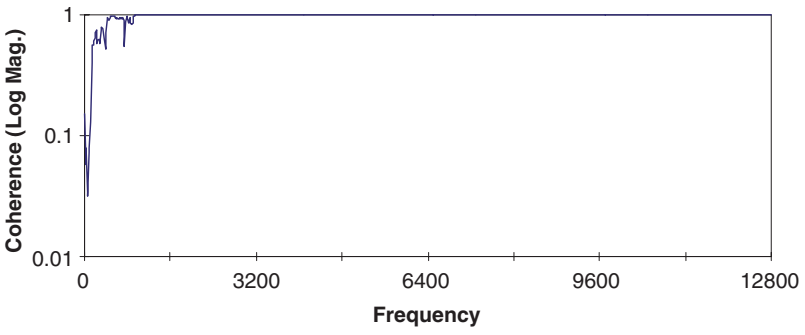

Fig. 16. Coherence between force and acceleration at input for big trapezoidal corrugated plate.

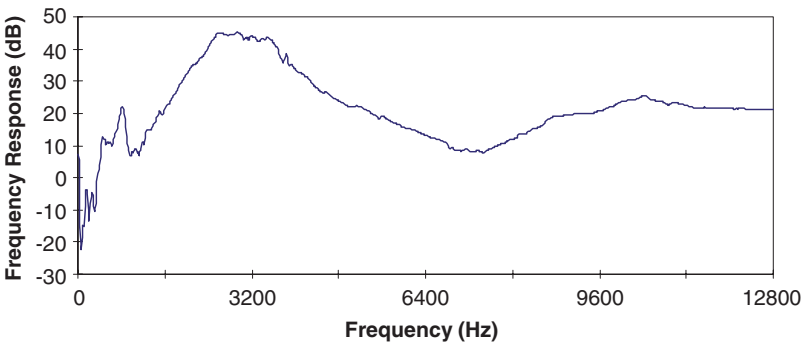

Fig. 17. Frequency response function of driving point acceleration (a/F) at input for small rectangular corrugated plate.

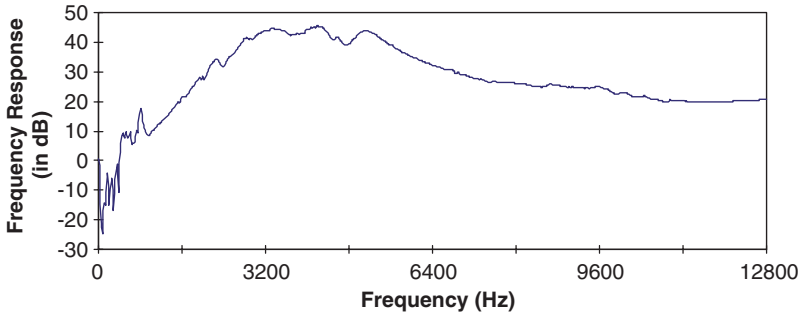

Fig. 18. Frequency response function of driving point acceleration (a/F) at input for small trapezoidal corrugated plate.

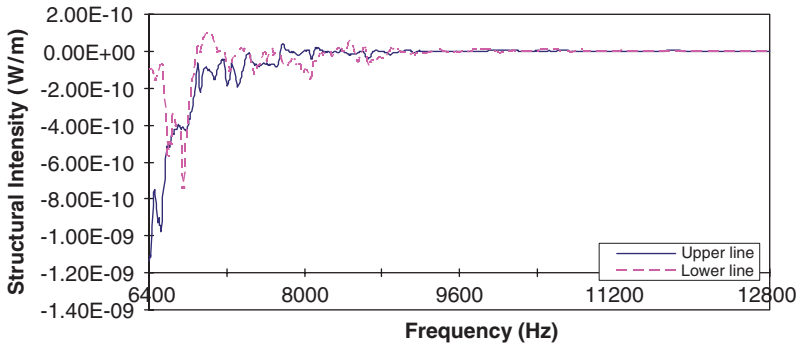

Fig. 19. Longitudinal wave power transmission for small rectangular corrugated plate.

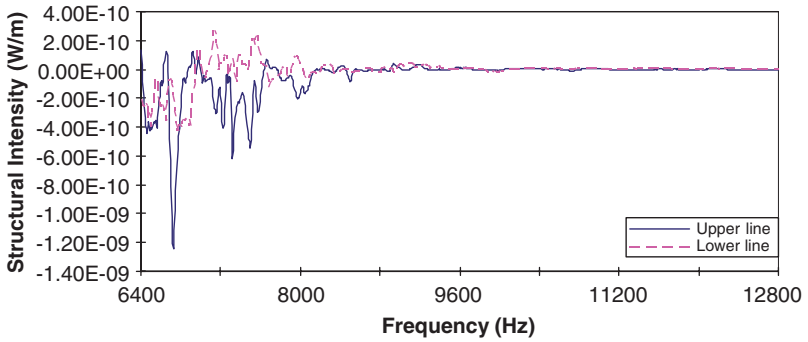

Fig. 20. Longitudinal wave power transmission for small trapezoidal corrugated plate.

physical plate's models of Ref. [5] to that of the present study, the magnitude of in-plane would be different. However, it may be possible to identify the trends of in-plane power transmission at high frequencies in both the cases. The results of in-plane power in Fig. 25 (log–log) and those from Figs. 23 and 24 yielded similar nature in the high-frequency range, maintaining nearly a constant magnitude. It is also observed from the present study that the controlling of in-plane at high frequency is difficult. On a qualitative basis, this comparison gives a good context of validation of the present study.

6. Results and discussions

As previously highlighted, although most works published in the literature were limited to simple beams and plates in bending, limited research on longitudinal wave is nevertheless available in isotropic plates. In this

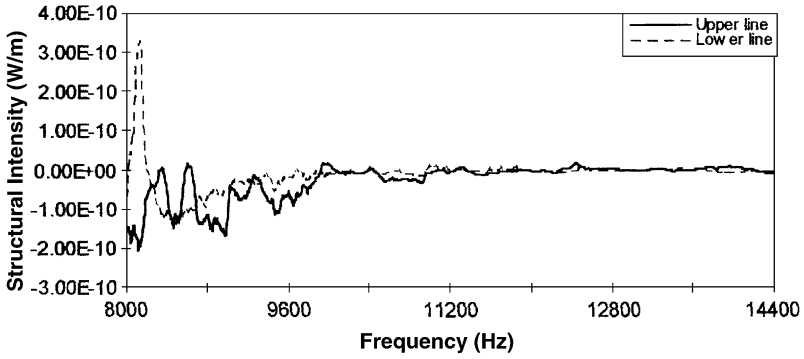

Fig. 21. Longitudinal wave power transmission for big rectangular corrugated plate.

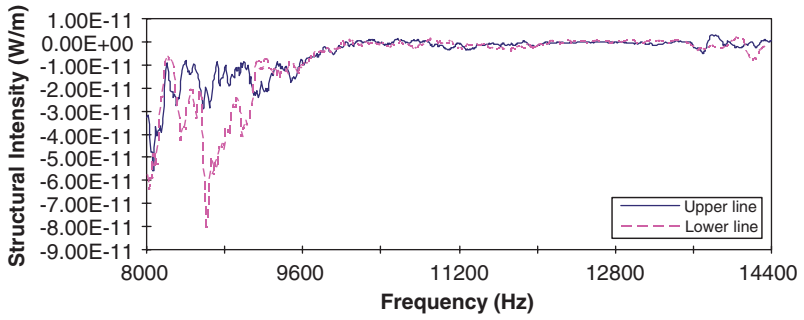

Fig. 22. Longitudinal wave power transmission for big trapezoidal corrugated plate.

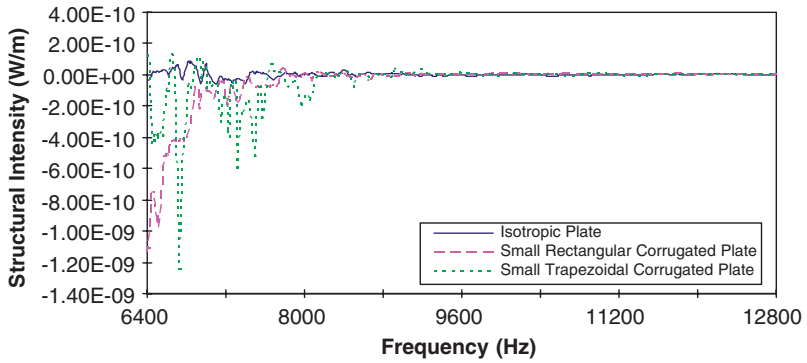

Fig. 23. Comparison of in plane power transmission from upper measurement line.

paper, quasi-longitudinal wave power was estimated first in isotropic plate to validate the test rig and measurement methodology. In these measurements a constant force signal to all plate models was provided so as to compare the results and to identify influences of longitudinal rigidity of the plates over power transmission. In this measurement, a mini-shaker is used for excitation of plates. A FFT analyzer (HP 35760A) was used to run the shaker. The noise generator of the FFT analyzer sent a constant random white noise with a level of 1.002 Vpk to the mini shaker to excite all the plates. The same internal setting for noise generation in FFT analyzer was maintained for all the cases.

Fig. 6 shows input in-plane force injected to the plates. In the frequency range 6.4–12.8 kHz, the value of force signal is shown to be stable and constant, consequently considered to be a white noise. The coherence

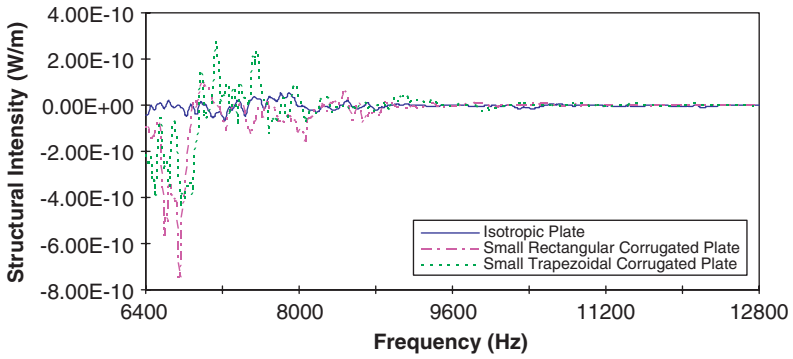

Fig. 24. Comparison in plane power transmission from lower measurement line.

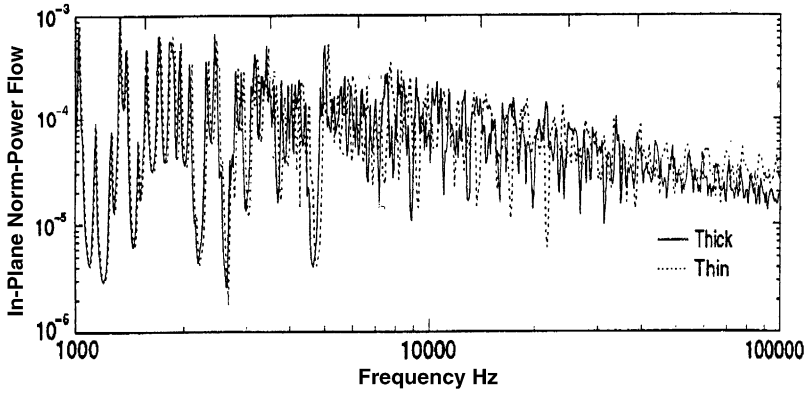

Fig. 25. In-plane power transmission in thick and thin L-shaped plate using SI [5].

function in Fig. 7 is also good. It is indicated that a little fluctuation occurs in very lower frequency but on an overall basis, it is deemed to be acceptable. Frequency response function (Fig. 8) of driving point acceleration depicts that the initial modes in the lower frequency range and modes in the higher frequency range of interest are more damped. Input power of isotropic plate is also measured in the frequency range of 0–12.8 kHz. Positives peaks at the lower frequency range were noted (Fig. 9). The results of quasi-longitudinal power in isotropic plate in Fig. 10 show a similar pattern to the results reported in literature [5] (Fig. 25, log–log scale). The values of longitudinal wave power obtained in Ref. [5] were larger in magnitude than those of the present study. It could be attributed to the fact of a higher input force level being injected to the plate. The results of the present study are however acceptable due to the similar results with Ref. [5] and thereby verified that the methodology and measurement set-up are applicable for measurement of quasi-longitudinal wave power in corrugated plates.

In the case of corrugated plates, coherence functions (Figs. 15 and 16), and driving point acceleration (Figs. 17 and 18) were measured and plotted. Extraneous noise in the signals sometimes yields uncorrelated output to input signals. An insufficient spectral resolution (Hz) also occasionally causes some lack of coherence at lower frequency range. The fluctuation in coherence functions in lower frequency range in Figs. 7, 15 and 16 may be due to noise. This trend can also be observed in the literature [13,15]. However on overall basis, it is not a problem and correlation between output to input signals can be trusted and is deemed acceptable [18]. In addition, for the frequency range of interest (6.4–12.8 kHz) the coherence value is unity, i.e. 100% correlated (Figs. 7, 15 and 16).

Driving point acceleration of these plates shows the similar nature to that of isotropic plate. Initial vibration modes and high-frequency vibration modes are more damped. But in the case of small rectangular corrugated

plate, few modes in the mid frequency range are more damped compared to those of trapezoidal corrugated plate. Input power for large frequency range was measured and plotted in Figs. 11–14. Few positives peaks of input power were observed. Quasi-longitudinal wave power was plotted in Figs. 19–22 for all corrugated plates which shows the similar results to those of Ref. [5]. There are some negatives peaks in the lower frequency range. It is also important to note that few negative peaks are nevertheless present in input power of these plates as well. The negative values of in-plane waves power measurement in this lower frequency range from lower measurement line were found to be smaller. This noticeable aspect of in-plane power transmission in corrugated plates can be explained further in the following.

Three influential aspects in this regard are: clamping of edges of the plate, vortex type and S-shaped power flow pattern. Two vertical sides of the plates were clamped by C-clamps (big and small) to obtain zero strain condition (as required for the model) in the direction perpendicular to the direction of clamped edges (Fig. 5). In real situation, it was relatively difficult to ensure a perfect zero strain in that direction. If some strain exists, this suggests that there would be some wave propagation in y-direction. Three types of power flow pattern [16] are observed: straight type, S-shaped type and vortex type. Among them, S-shaped type and vortex type flow pattern may play important roles for energy transfer especially in making negatives loops. These patterns are applicable to in-plane waves. This is also true for acoustic intensity [16]. Due to the combining effects of these aspects, in some frequencies, negative values of power from both measurement lines were estimated. However, the reasons for negative input power of plates at a few frequencies cannot be explained precisely at this stage.

A similar nature of vibration power could be observed from Figs. 19–22. In some frequencies, power transmission from both lower measurement line and upper measurement line indicates a distorted (not similar) fluctuation pattern. It may be because of reflections and scattering of waves from the clamp edges and not fully one-directional power flowing towards the damping region. This is another aspect of occuring negative peaks in energy transfer. From these figures, it is also clear that power measuring from upper line is conservative in some frequencies. Power was measured from a line grid, selecting a few points on a line. It may be possible that these few selected measurement points on the upper line have low energy flux. It is possible that points with high energy flux were not considered. When averaging the power, considering all these selected points on the upper line could give a lower value compared to that of lower line (Fig. 5). More points on each line may solve this issue.

It is also seen another aspect of in-plane wave from input power and transmitted power at very high frequencies. There is a negligible amount of energy present in those frequencies. This is due to the fact that most of vibration modes in the higher frequency range are more damped and have lower input excitation. Consequently, it may be argued that at high frequencies it very difficult to excite quasi-longitudinal waves.

In-plane wave power was compared to analyze the effect of longitudinal stiffness due to corrugation. It was observed that the power flow reduced gradually as frequency increases with some waviness in the initial frequency range. At the higher frequency range, no significant variation of the values of the estimated power was observed. The values mostly remained constant and stable. This similar pattern of constant magnitude of average in-plane power is seen in the literature (Fig. 25) [5]. The waviness of in-plane power was noticed but maintaining a constant average magnitude (Fig. 25). It was also detected from this study that there was no significant effect of longitudinal stiffness on power flow in general. The pattern and magnitude of power flow in isotropic plates and trapezoidal corrugated plates for quasi-longitudinal waves were similar except for lower frequency range, suggesting that longitudinal stiffness produced insignificant contribution on power flow by quasi-longitudinal wave at the higher frequency range. This effect of longitudinal stiffness on in-plane power transmission could be observed from Figs. 23 and 24. This result suggests that quasi-longitudinal wave power could not be controlled by increasing the longitudinal stiffness. For flexural waves, on the other hand, increasing flexural rigidity is a good way to suppress vibration [15]. Therefore, for in-plane waves other vibration control methods such as surface treatment may be employed.

To provide a fixed boundary condition (BC) is a big challenge for instrumentation engineers. Unlike the fixed BC, simple supported BC, for example, is quite easy to achieve. Twelve big C-clamps were employed on each side of the plate and tightened those very hard with a fixed support. In addition, few small C-clamps were also used in between the big clamps. As many hard tight C-clamps (big and small) are employed on each side, it can be trusted that a zero strain in y-direction may be attained. Similarity of the results of present study and that available in literature [5] can further increase the belief that a zero strain was obtained in the y-direction.

Bee-wax is a conventional use in vibration transducer attachment to the structures. It is useful both in flexural and in-plane wave vibrations. A thin layer of bee-wax was used to connect accelerometers to the plates. As the frequency contents at higher range of the present study are mostly similar to that in the literature [5], it can be expected that the influences of bee-wax on vibration behavior and energy transfer would be minimal at the high-frequency range. However, accuracy of results due the application of bee-wax, accelerometer loading, transducer cables, finite difference and phase mismatch errors are beyond the scope of the paper. Linjama [18] and Shibata et al. [19] investigated error analysis in vibration measurements. In this study, uncoupled in-plane wave was considered separately. Bending wave vibration was not therefore checked under longitudinal excitation. A related work of error estimation of bending wave power flow in presence of in-plane wave was reported before Ref. [9]. Mode shapes of the plates for resonant peaks could not be identified as this was beyond the scope of this work.

7. Conclusions

Developed measurement was used to estimate quasi-longitudinal wave power in corrugated plates. Method of elastic equivalence was used to model the corrugated plates. The established method as used for an isotropic plate was used to validate the methodology. Both input power and power flowing through the plates were presented. In-plane power transmission from isotropic plate, small rectangular and trapezoidal corrugated plates was compared. For big rectangular and trapezoidal corrugated plates, this type of comparison was not carried out because of different frequency limits. Power estimations from isotropic plate and other small corrugated plates indicated that the increasing longitudinal stiffness is not an effective way to suppress in-plane vibration. Except at some lower part of the frequency range of interest, the results of quasi-longitudinal wave power from both isotropic plate and corrugated plates are nearly the same, suggesting that other vibration control methods should be considered to control in-plane waves.

Reference

[1] A.C. Nilsson, Attenuation of Structure-borne Sound in Superstructures in Ships, *Journal of Sound and Vibration* 55 (1977) 71–91.
[2] B.M. Gibbs, C.L.S. Gilford, the Use of Power Flow Methods for the Assessment of Sound Transmission in Building Structures, *Journal of Sound and Vibration* 49 (1976) 267–286.
[3] A. E. Landmann, H. F. Tillema, S. E. Marshall, evaluation of Analysis Techniques for Low Frequency Interior Noise and Vibration of Commercial Aircraft, NASA-CR-181851, 1989.
[4] D.H. Park, S.Y. Hong, H.G. Kil, J.J. Jeon, Power Flow Models and Analysis of In-Plane Waves in Finite Coupled Thin Plates, *Journal of Sound and Vibration* 244 (4) (2001) 651–668.
[5] J.M. Cuschieri, M.D. McCollum, In-plane and out-of-plane waves power transmission through an L-type junction using mobility power flow approach, *Journal of the Acoustical Society of America* 100 (2) (1996) 857–870.
[6] R.H. Lyon, in-Plane contribution to Structural Noise Transmission, *Journal of Noise Control Engineering* 26 (1986) 22–27.
[7] A.N. Bercin, an assessment of the Effects of In-Plane Vibrations on the Energy Flow between Coupled Plates, *Journal of Sound and Vibration* 191 (5) (1996) 661–680.
[8] B.M. Gibbs, P.G. Craven, Sound transmission and mode coupling at junctions of thin plates, part II: parametric survey, *Journal of Sound and Vibration* 77 (1981) 429–435.
[9] K.Q. Kay, D.C. Swanson, Error in bending wave power measurements resulting from longitudinal waves, *Noise Control Engineering Journal* 44 (4) (1996) 185–192.
[10] R.J.M. Craik, A. Thancanamootoo, Applications of the Dynamic Stiffness Method to the free and forced vibrations in Aircraft Structures, *Applied Acoustics* 37 (2) (1992) 85–109.
[11] L. Cremer, M. Heckl, *Structure-borne Sound: Structural Vibration and Sound Radiation at Audio Frequencies*, Springer, Berlin, 1988.
[12] N.K. Mandal, M.S. Leong, RAbd. Rahman, Measurement of quasi-longitudinal wave power in thin single-layer naturally orthotropic plates, *International Journal of Acoustics and Vibration* 5 (2) (2000) 106–108.
[13] J. Linjama, T. Lathi, Estimation of bending wave intensity in beams using the frequency response technique, *Journal of Sound and Vibration* 153 (1) (1992) 21–36.
[14] M.S. Troitskey, *Stiffened Plates: Bending, Stability and Vibration*, Elsevier Scientific Publishing Company, Amsterdam, 1976.
[15] N.K. Mandal, R.A. Rahman, M.S. Leong, experimental Investigation of Vibration Power Flow in Thin Technical Orthotropic Plates by the Method of Vibration Intensity, *Journal of Sound and Vibration* 285 (3) (2005) 669–695.
[16] N. Tanaka, Vibration and acoustic power flow of an actively controlled thin plate, *Noise Control Engineering Journal* 44 (1) (1996) 23–33.

[17] M.S. Khun, H.P. Lee, S.P. Lim, Structural intensity in plates with multiple discrete and distributed spring-dashpot systems, *Journal of Sound and Vibration* 276 (2004) 627–648.
[18] J. Linjama, Propagation of mechanical vibration in structures, experimental development of the vibration intensity method, VTT Publication 170, Technical Research Centre of Finland, 1994.
[19] K. Shibata, M. Kato, N. Takatsu, O. Wakatsuki, K. Kobayashi, Measuring condition and precision of structural intensity, *Proceeding of Inter-Noise* 94, 1994, pp. 1697–1700.